4322–4330 *Nucleic Acids Research, 2007, Vol. 35, No. 13* *Published online 18 June 2007*
doi:10.1093/nar/gkm437

A systematic analysis of the effect of target RNA structure on RNA interference

Ellen M. Westerhout and Ben Berkhout*

Laboratory of Experimental Virology, Department of Medical Microbiology, Center for Infection and Immunity Amsterdam (CINIMA), Academic Medical Center, University of Amsterdam, The Netherlands

Received January 9, 2007; Revised and Accepted May 16, 2007

ABSTRACT

RNAi efficiency is influenced by local RNA structure of the target sequence. We studied this structure-based resistance in detail by targeting a perfect RNA hairpin and subsequently destabilized its tight structure by mutation, thereby gradually exposing the target sequence. Although the tightest RNA hairpins were completely resistant to RNAi, we observed an inverse correlation between the overall target hairpin stability and RNAi efficiency within a specific thermodynamic stability (ΔG) range. Increased RNAi efficiency was shown to be caused by improved binding of the siRNA to the destabilized target RNA hairpins. The mutational effects vary for different target regions. We find an accessible target 3′ end to be most important for RNAi-mediated inhibition. However, these 3′ end effects cannot be reproduced in siRNA-target RNA-binding studies *in vitro*, indicating the important role of RISC components in the *in vivo* RNAi reaction. The results provide a more detailed insight into the impact of target RNA structure on RNAi and we discuss several possible implications. With respect to lentiviral-mediated delivery of shRNA expression cassettes, we present a ΔG window to destabilize the shRNA insert for vector improvement, while avoiding RNAi-mediated self-targeting during lentiviral vector production.

INTRODUCTION

RNA interference (RNAi) is induced by double-stranded RNA (dsRNA) and results in gene silencing through sequence-specific degradation of the target RNA (1). RNAi provides plants and animals a defense mechanism against viruses (2–4) and retrotransposons (5,6). The ribonuclease Dicer processes the long dsRNA replication intermediates into small interfering RNAs (siRNAs) of ~22 nucleotides (nt) (7–9). These siRNAs are incorporated into the RNA-induced silencing complex (RISC) that finds complementary RNA sequences, resulting in cleavage of the target RNA (10,11). The central catalytic component of RISC is an Argonaute protein, which contains the signature domains PAZ and PIWI responsible for binding the siRNA strand (12).

Transfection of synthetic siRNAs into cells or intracellular expression of short hairpin RNAs (shRNAs), which are processed into siRNA duplexes by Dicer, are powerful tools to suppress gene expression (13–15). Randomly selected siRNAs against a target show a large variation in their efficacy (16). Empirical rules on siRNA duplex features have been reported and improve design of effective siRNAs. The asymmetry rule for siRNA duplex ends requires that the 5′ end of the antisense strand forms a less stable end with its complement than the 5′ end of the sense strand (17,18). Related to this rule is the described requirement of high A/U content at the 5′ end of the antisense strand and high G/C at the 5′ end of the sense strand (19,20). In addition, a number of position-specific nucleotides, an unstructured guide-RNA, and an accessible target site have been reported to positively effect siRNA efficiency (19,21–23).

RNAi can be used as a therapeutic strategy against human pathogenic viruses such as HIV-1 (24). HIV-1 replication can be inhibited transiently by transfection of synthetic siRNAs targeting viral RNA sequences or cellular co-factors (25–28). Furthermore, long-term inhibition of HIV-1 replication has been demonstrated in transduced cell lines stably expressing antiviral siRNAs or shRNAs (29–34). However, HIV-1 escape variants with nucleotide substitutions or deletions in the siRNA target sequence do emerge after prolonged culturing (31,35,36). The emergence of RNAi-resistant variants may be blocked by a combination-shRNA therapy, which simultaneously targets multiple conserved viral RNA sequences (34,37).

We demonstrated that HIV-1 can also become resistant against RNAi by placing the target sequence in a stable

*To whom correspondence should be addressed. Tel: +31 20 566 4822; Fax: +31 20 691 6531; Email: b.berkhout@amc.uva.nl

© 2007 The Author(s)
This is an Open Access article distributed under the terms of the Creative Commons Attribution Non-Commercial License (http://creativecommons.org/licenses/by-nc/2.0/uk/) which permits unrestricted non-commercial use, distribution, and reproduction in any medium, provided the original work is properly cited.

RNA structure, which prevents binding of the siRNA (36). We also suggested that such structure-based target occlusion occurs in the RNA genomes of lentiviral vectors with a shRNA-cassette (59). By inserting these cassettes, the target sequence will automatically be present in the vector genome, and self-targeting by the shRNA should reduce the lentiviral production level. However, since the target sequence in the genome is also located in this perfect shRNA hairpin, it is protected against RNAi, ensuring a normal vector titer. Indeed, when the target in the lentiviral genome is unstructured, the titer is significantly reduced by the shRNA (38).

The inhibitory effect of target RNA structure on RNAi efficiency has been described in several studies (23,39,40). These studies compared the efficiency of different siRNAs on a fixed target, and found a correlation between target availability and RNAi efficiency. Schubert *et al*. suggested that the local free energy of base pairing in the target region determines RNAi efficiency (41). Ideally, one should test this concept by a mutational analysis of one target instead of comparing different siRNAs with intrinsically different RNAi efficacies. In this scenario, mutations that affect the RNA structure should not affect the target sequence itself, such that the same siRNA inhibitor can be used. In this study, we set out to determine the exact hairpin stability at which RNAi suppression occurs by systematically destabilizing a 21-base pair (bp) hairpin structure that occludes the complete target sequence. We monitored the effects on siRNA binding *in vitro* and RNAi efficiency *in vivo*. The 3′ end of the mRNA target sequence is initially recognized by bases 2–5 of the antisense/guide strand siRNA, therefore named the 'seed' sequence (42,43). Thus, one may expect a more prominent effect of an accessible target 3′ end, which primed us to address positional effects when destabilizing the target hairpin. The results demonstrate a clear correlation between the overall stability of the target hairpin and RNAi efficiency, but positional effects were also apparent.

MATERIALS AND METHODS

Plasmid constructs

The luciferase plasmids pGL3-wt, pGL3-T1 to pGL3-T7 (Figure 1B) and pGL3-A to pGL3-G (Figure 3A) were constructed by annealing of forward (fwd) and reverse (rev) oligonucleotides (Supplementary Data, Table 1) and ligation into the EcoRI and PstI sites of the firefly luciferase expression vector pGL3-Nef (36). The pSUPER-shPol vector (34) encodes an effective shRNA against a conserved 19-nt HIV-1 region (Pol1; ACAGGAGCAGAUGAUACAG) under the control of an H1 polymerase III promoter (13). The plasmid pRL-CMV (Promega) expresses Renilla luciferase under control of the CMV promoter.

Cell culture and luciferase assays

C33A cervix carcinoma cells were grown as a monolayer in Dulbecco's modified Eagle's medium supplemented with 10% FCS, minimal essential medium nonessential amino acids, 100 units/ml penicillin, and 100 units/ml streptomycin at 37°C and 5% CO_2. C33A cells were grown in 1 ml culture medium in 2 cm^2 wells to 60% confluence and transfected by the calcium phosphate method. The pGL3-variant (100 ng) was mixed with 0.5 ng pRL-CMV, 0.1–100 ng pSUPER-shPol and pBluescriptII (KS^+) (Stratagene) to have 1 μg of DNA in 15 μl water. The DNA was mixed with 25 μl of 2× HBS and 10 μl of 0.6 M $CaCl_2$, incubated at room temperature for 20 min and added to the culture medium. The culture medium was refreshed after 16 h, and cells were lysed after another 24 h. Firefly and Renilla luciferase activities were measured with the Dual-luciferase Reporter Assay System (Promega) as described previously (36).

RT-PCR

C33A cells (2 cm^2) transfected with 100 ng pGL3-variants and 0 or 10 ng pSUPER-shPol were lysed 2 days after transfection. Total RNA was isolated with TRIZOL® reagent (Invitrogen) according to the manufacturer's protocol. Contaminating genomic DNA was removed by DNase treatment using the TURBO DNA-free™ kit (Ambion). First strand cDNA was synthesized using 1 μg of total RNA, Thermoscript™ reverse transcriptase (Invitrogen), and primers. The gene-specific primers used were EWr6 (5′-GCCCCGACTCTAGACTGCAG-3′) for Firefly luciferase and 3′HC-b-ACTIN (5′-TGTGTTGGCGTACAGGTCTTTG-3′) for actin.

PCR amplification (25 cycles) was performed on 2, 0.4, 0.08 or 0.016 μl RT product with Firefly luciferase primers EWr6 and GL3pcr-RT (5′-GCTGAATTGG AAT-CCATCTT-3′) or actin primers 3′HC-b-ACTIN and 5′HC-b-ACTIN (5′-GGGAAATCGT-GCGTGA CATTAAG-3′). The PCR products, respectively 398 and 275 bp, were run on a 1.5% agarose gel.

In vitro transcription and electrophoretic mobility shift assay (EMSA)

The pGL3-variant plasmids were used as template for PCR amplification with primers EWr8 (5′-TCC*TAATACGACTCACTATAGG*TTCCCCACAGGA GCAGATGA-3′; T7 RNA-polymerase promoter in italics) and EWr9 (5′- GACTCTAGACTGCAGAAAAC -3′). The resulting PCR product contains a T7 RNA-polymerase promoter upstream of the hairpin (hairpin nt underlined). DNA products were purified from agarose gel using QiaexII Gel extraction kit (Qiagen). RNA transcripts were produced by *in vitro* transcription with the Megashortscript T7 transcription kit (Ambion), and transcripts were checked for integrity and isolated from an 8% acrylamide gel. RNA concentrations were determined by spectrophotometry.

The siRNA-Pol antisense/guide oligonucleotide CUGUAUCAUCUGCUCCU-GU (Eurogentec) was 5′ end labeled with the kinaseMax kit (Ambion) and 1 μl [γ-^{32}P] ATP (0.37 MBq/μl, Amersham Biosciences). The target hairpin RNAs were denatured in 30 μl water at 85°C for 3 min followed by snap cooling on ice. After addition of 10 μl 4× MO buffer (final concentration: 125 mM KAc, 2.5 mM MgAc, 25 mM HEPES, pH 7.0),

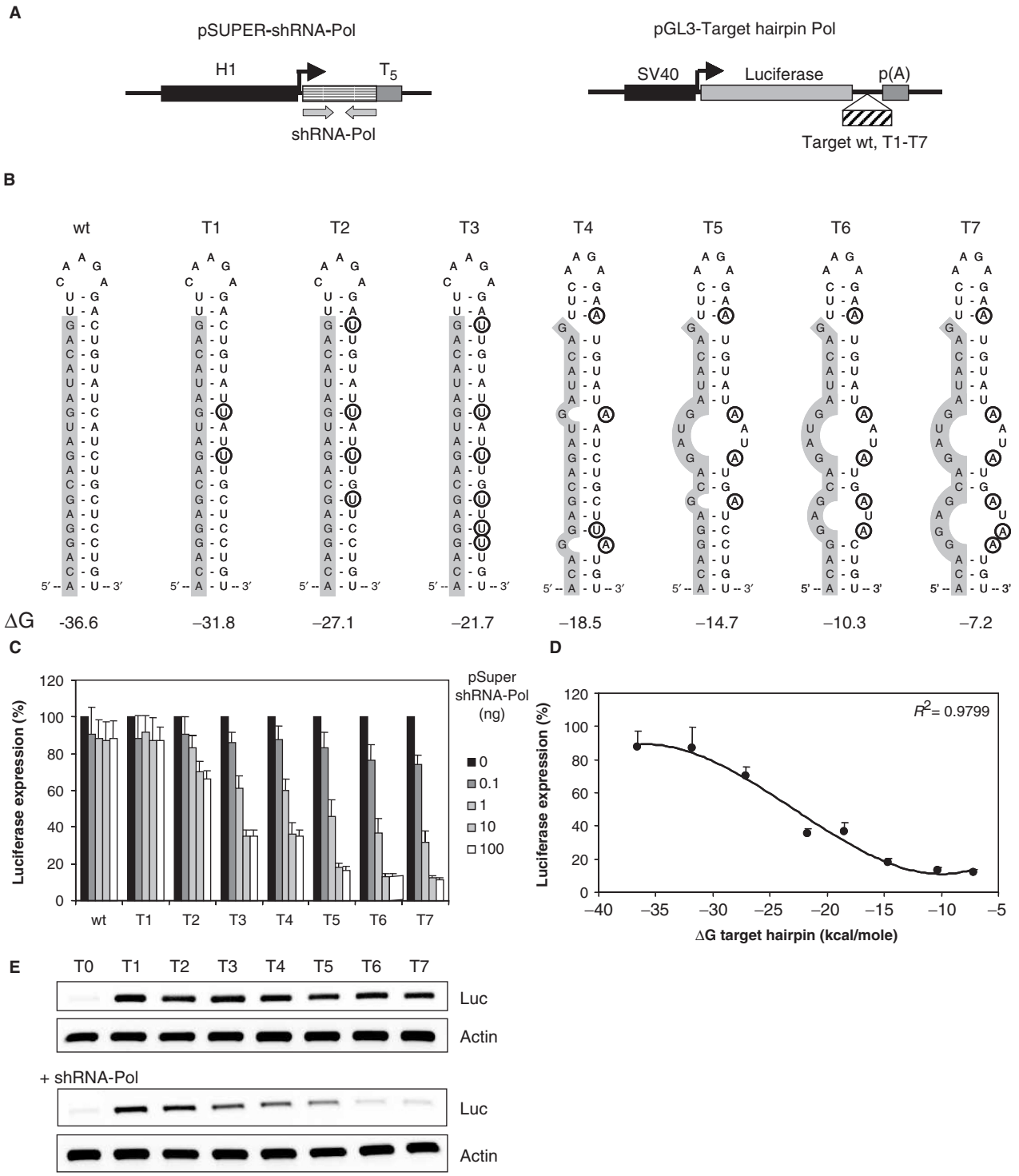

Figure 1. Target RNA structure influences RNAi efficiency. (**A**) The HIV-based target sequences (54 nt) were cloned downstream of the firefly luciferase gene in the pGL3 reporter plasmid. These reporter constructs were co-transfected into C33A cells with the shRNA expressing plasmid pSUPER-shRNA-Pol. The respective H1 (polymerase III) and SV40 (polymerase II) promoter units are indicated by a black box, the arrow marks the transcription initiation site. (**B**) The predicted RNA structures (Mfold program) of the wild-type (wt) shPol and mutated hairpins (T1–T7). The 19-nt target sequence is highlighted as a gray box and the mutated nucleotides are encircled. The thermodynamic stability (ΔG in kcal/mol) of the target hairpins is indicated (54 nt total; CCCC + indicated hairpin + UUU). (**C**) Luciferase expression upon transfection of the reporter constructs with increasing amounts of pSUPER-shRNA-Pol. The firefly luciferase activity was normalized to that of the Renilla luciferase to correct for variation in transfection efficiency. The level of expression observed in the absence of shRNA-Pol was set at 100% for each reporter construct. This level did not vary significantly for the different constructs. The mean values of six independent experiments are shown (±SD). (**D**) The thermodynamic stability of the target hairpins is plotted against the level of luciferase expression as observed in Figure 1C with 10 ng pSUPER-shRNA-Pol. (**E**) Semi-quantitative RT-PCR on RNA isolated from cells transfected with 100 ng pGL3-target hairpin variants with or without 10 ng pSUPER-shRNA-Pol. Actin levels serve as a control.

the RNA was renatured at 37°C for 30 min. The transcripts were diluted in 1× MO buffer to a final concentration varying from 0 to 1.0 μM in MO buffer. Unlabeled tRNA (1 μg) was added as competitor to each reaction to minimize aspecific RNA interactions. The 5′-labeled oligonucleotide (1.0 nM) was added and the samples (20 μl) were incubated for 30 min at 37°C. After adding 4 μl non-denaturing loading buffer (50% glycerol with bromophenol blue), the sample was analyzed on a non-denaturing 4% acrylamide gel. Electrophoresis was performed at 150 V at room temperature and the gel was subsequently dried. Quantification of the free and bound oligonucleotide was performed with a Phosphor Imager (Molecular Dynamics).

In silico RNA analysis

The structure and stability of the target hairpins cloned into the pGL3-variants was predicted with the RNA Mfold program (44,45) at http://www.bioinfo.rpi.edu/applications/mfold. The indicated ΔG in Figure 1B and Figure 3A are derived by importing the hairpin sequences into the program (54 nt total: 5′ CCCC + hairpin sequences + UUU) and did not contain luciferase sequences. The presence of the predicted hairpin structures in the context of the luciferase reporter construct was verified by importing longer sequences (150 nt total; 52 nt + hairpin sequences + 51 nt) into Mfold.

RESULTS

Target hairpin destabilization triggers RNAi

We investigated the effect of target RNA structure on RNAi efficiency. As a model system we used a very potent shRNA inhibitor that is directed against the Pol gene of HIV-1 (Figure 1A; left) and that has been tested extensively against HIV-1 and appropriate reporter genes (34). Such a luciferase reporter with the HIV-1 Pol target sequence in the 3′ UTR is shown in Figure 1A (right). Next, we made the target inaccessible by inclusion in a perfect hairpin of $\Delta G = -36.6$ kcal/mol (Figure 1B; wild type (wt), the target sequence is marked in gray). In fact, this hairpin structure is identical to the shRNA itself. The top 2 bp and the 5-nt loop are standard in the optimized pSUPER system (13). We systematically destabilized this target hairpin in mutants T1–T7 by introducing nt substitutions in the descending strand of the stem (encircled in Figure 1B), thus leaving the target sequence intact. The mutations were chosen such that the predicted thermodynamic stability (ΔG) decreases gradually. We first destabilized the hairpin by replacing stable G-C by weak G-U base pairs (mutants T1–T3), followed by more gross destabilizations, e.g. by introducing mismatches (mutants T4–T7). The ΔG value was reduced in a step-wise manner to −7.2 kcal/mol for mutant T7.

To accurately quantify the RNAi efficiency against these differentially structured targets, we placed them downstream of the luciferase reporter gene (Figure 1A; right). These constructs were co-transfected into cells with increasing amounts of the shRNA-Pol expression vector and luciferase expression was measured after 48 h (Figure 1C). Expression of the reporter construct with the target sequence embedded in the wt hairpin was completely resistant against shRNA-Pol. The same expression pattern was observed for the T1 construct, but T2 already showed some susceptibility for RNAi-mediated inhibition with higher amounts of shRNA-Pol, with a maximal inhibition of 34% (66% residual luciferase expression). The next reporter constructs (T3,T4) showed a significant drop in luciferase expression (64% inhibition). Inhibition of the remaining destabilized target hairpins (T5–T7) was very effective, showing more than 80% inhibition. This is similar to the maximal inhibition level that can be obtained with this potent shRNA inhibitor against a reporter with the 19-nt target sequence in an unstructured setting [(34) and results not shown]. To verify that the reduction of luciferase expression is due to mRNA degradation, we performed a semi-quantitative RT-PCR on cellular RNA (Figure 1E). Consistent with the luciferase assays, the levels of mRNA are increasingly diminished for transfections with the constructs T2 to T7 and shRNA-Pol. The near absence of PCR product for construct T0, with or without shRNA-Pol, indicates an inefficient RT reaction through a perfect hairpin. There were no PCR products when RNA was used as input for the PCRs (results not shown).

We plotted the measured level of luciferase expression against the predicted stability of the target hairpins (Figure 1D). The results suggest an inverse linear correlation between RNAi-susceptibility and target hairpin stability in the −30/−15 kcal/mol range. The curve shows two plateaus. A reduction in hairpin stability from −36 to −30 kcal/mol does not significantly induce RNAi-mediated inhibition (<20% inhibition), and further destabilization above −15 kcal/mol shows no significant improvement of the already maximal inhibition of ∼86%.

Target hairpin destabilization triggers siRNA binding

To demonstrate that the increased RNAi efficiency on destabilized target hairpins is due to more efficient binding of the siRNA, we performed *in vitro* binding experiments by means of electrophoretic mobility shift assays (EMSA). For this, we used short T7 transcripts with the complete hairpin and a 19-nt RNA oligonucleotide, which corresponds to the antisense/guide strand of the siRNA-Pol (complementary to boxed sequence in Figure 1B). The siRNA was radioactively labeled and incubated with increasing amounts of target transcript (wt, T1–T7), and subsequently analyzed on a non-denaturing acrylamide gel (Figure 2A). Binding of siRNA to the target RNA leads to duplex formation that results in a band shift on the gel. Unbound siRNA and the siRNA/target RNA duplex were quantified to calculate the percentage of binding (Figure 2B).

We performed the binding experiment multiple times with 0.2 μM target RNA because efficient binding can be observed, yet most variants stay within the linear range of the binding assay. We plotted these binding percentages against the predicted stability of the target hairpins (Figure 2C). A general trend can be observed that is the opposite of the graph in Figure 1D: reduced hairpin

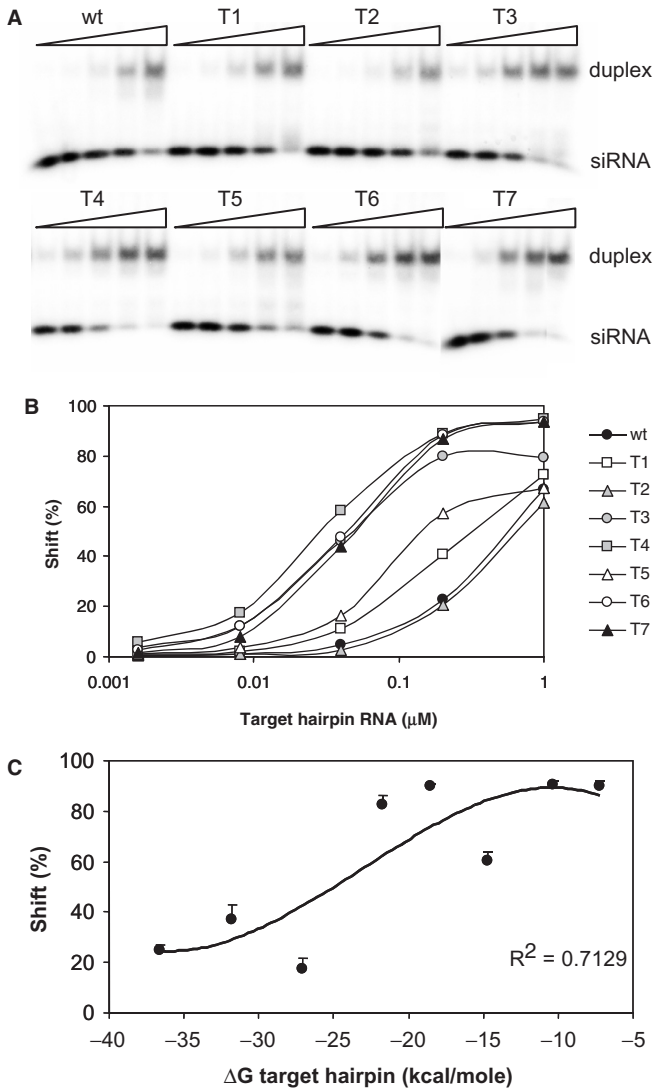

Figure 2. Target RNA structure influences siRNA binding. (**A**) Radioactively labeled oligonucleotide simulating the siRNA antisense strand (processed from shRNA-Pol) was incubated with increasing amounts of hairpin target RNA variants (wt, T1–T7). SiRNA/target RNA duplex formation was analyzed by EMSA. (**B**) Free and bound siRNA oligonucleotide was quantified to calculate the level of duplex formation (bound siRNA/free + bound siRNA). (**C**) The thermodynamic stability of the target hairpins is plotted against the level of duplex formation with 0.2 μM target RNA.

stability results in more efficient binding of the siRNA to the target RNA. Thus, a decrease in the stability of the target hairpin increases RNAi efficiency due to more efficient binding of the siRNA. The largest improvement in RNA–RNA interaction and RNAi efficiency is observed for mutant T3 in comparison with T2, indicating that a threshold stability is passed by going from $\Delta G = -27.1$ to -21.7 kcal/mol.

Accessibility of the 3′ end of the target sequence is beneficial for RNAi

We globally determined the stability at which hairpin structures become inhibitory to the RNAi machinery. However, not all domains within the 19-nt target sequence may contribute equally to siRNA binding and the RNAi mechanism. For instance, it has previously been suggested that the 3′ end of the target sequence is initially recognized by the siRNA within RISC (43). To test this, we made a second set of Luc-target constructs (Figure 3A, mutants A–G). By introducing clustered mutations in the target hairpin, we destabilized either the 3′ end, the center or the 5′ end of the target sequence. Modest G-U changes were introduced in mutants A (3′), B (center) and C (5′). More gross destabilizing mutations were introduced in mutants D (3′), E (center) and F (5′). However, it is apparent that the two mutations in D have a more modest effect on the ΔG value because a realignment of the sequences trigger an alternative folding of the top of the hairpin. We therefore constructed the additional mutant G with three mutations to obtain a hairpin with a destabilized 3′ target end that is comparable in ΔG to hairpins E and F. Target hairpins A through G were cloned in the luciferase reporter and co-transfected into cells with increasing amounts of the shRNA-Pol expression vector to quantify the RNAi efficiency (results not shown).

The luciferase values obtained with 10 ng shRNA-Pol were plotted against the predicted hairpin stability (Figure 3B, left) and we zoom in on a smaller ΔG range (Figure 3B; right graph). The target hairpins A, B and C follow the general trend that we described previously (gray dotted trend line). Independent of where the hairpin is destabilized, the introduction of G-U base pairs is a too modest manipulation to trigger RNAi activity. The target hairpins E, F and G have more dramatic changes that reduce the overall hairpin stability to $-25/-26$ kcal/mol, which should become susceptible to RNAi according to the previous results. However, mutants F (5′) and E (center) remain largely insensitive, but mutant G with a free 3′ end shows increased RNAi sensitivity when compared to the trend line. Even the D mutant with a more modest destabilization of the target 3′ end shows reasonable RNAi activity and clearly drops below the trend line. These results confirm the importance of initial recognition of the 3′ target end, which explains the deviations from the general trend.

In vitro siRNA-target RNA binding does not accurately mimic the RNAi mechanism

We performed *in vitro* binding experiments to study the A–G mutants for their ability to bind the siRNA. The radioactively labeled siRNA was incubated with increasing amounts of the target transcripts A–G and analyzed on gel (Figure 4A). The shifts representing the siRNA/target RNA duplex and the free siRNA bands were quantified to calculate the percentage of binding (Figure 4B).

The percentage of binding with 0.2 μM target RNA was plotted against the predicted stabilities of the target hairpins (Figure 4C). Remarkably, these *in vitro* binding results differ significantly from the *in vivo* RNAi results. The target hairpins D and G (both 3′), which are efficiently targeted by RNAi in the luciferase assay (Figure 3B), are inefficient in siRNA binding. In contrast, the target

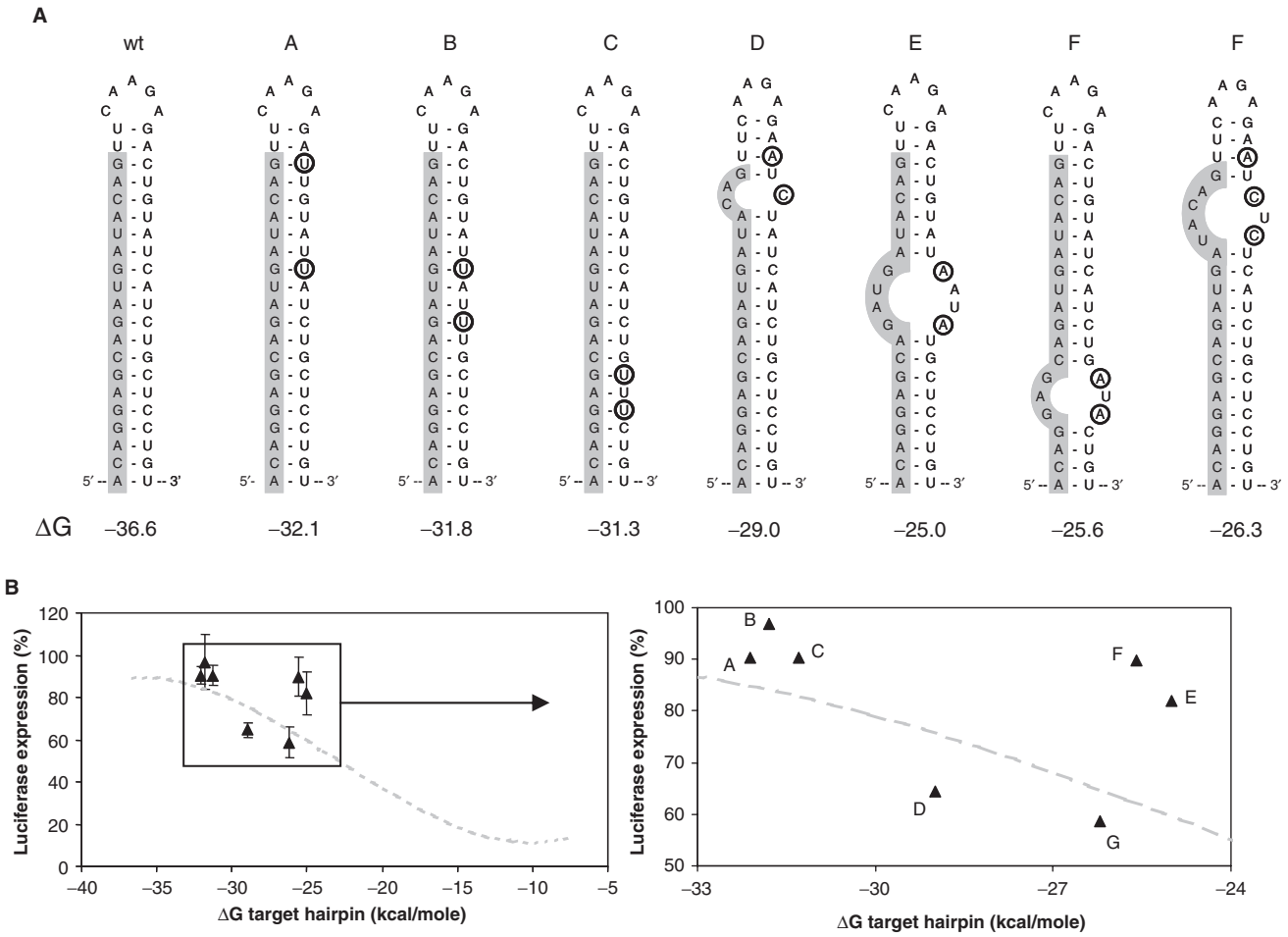

Figure 3. Position-specific destabilization of target hairpin triggers RNAi differentially. (**A**) Predicted RNA structures of the wt and mutant hairpins A–G. The target sequence is highlighted in the gray box and the mutated nucleotides are encircled. The thermodynamic stability (ΔG in kcal/mol) of the target hairpins is provided for each structure (54 nt total; CCCC + indicated hairpin + UUU). (**B**) Luciferase expression observed after transfection of the reporter constructs with 10 ng pSUPER-shRNA-Pol is plotted against the thermodynamic stability of the target hairpins. The

hairpins F (5′) and G (center) showed a slightly increased binding efficiency, although these construct were relatively more RNAi resistant in the luciferase assay. These results may reflect the oversimplification of the *in vitro* binding assay and point to a contribution of the RISC/siRNA complex in the recognition and binding of the target sequence *in vivo*.

DISCUSSION

It has been proposed that RNAi efficiency is influenced by the local RNA structure of the targeted sequence. We investigated this phenomenon in detail by placement of the target sequence in a perfect hairpin structure ($\Delta G = -36.6$ kcal/mol), which indeed resisted RNAi. Subsequently we destabilized this tight target structure resulting in a gradual exposure of the target sequence. Destabilization of the hairpin structure has little effect on RNAi activity until a threshold is reached ($\Delta G \approx -30$ kcal/mol). Beyond this threshold we demonstrate an inverse correlation between hairpin stability and RNAi-mediated inhibition. Maximal RNAi efficiency was observed with hairpins of $\Delta G \geq -15$ kcal/mol. *In vitro* binding experiments suggested that the increase of RNAi-mediated inhibition is due to efficient siRNA binding to the destabilized target RNA hairpins.

When we introduced position-specific mutations in the target hairpin, we observed RNAi efficiencies that deviate from this trend. Hairpins with an opened 5′ end or central part of the target sequence show less RNAi activity than predicted based on their overall stability. In contrast, hairpins with an opened 3′ end are more susceptible to RNAi than expected. These results are consistent with the current notion that the 3′ region of the target is initially recognized and bound by the RISC/siRNA complex (43). This model is supported by structural data on RISC bound to the siRNA strand. The 3′ end of the siRNA is recognized and bound in a pocket by the PAZ domain of the Argonaute protein (46). The 5′ end of the siRNA is anchored at the PIWI domain of Argonaute and these 5′ nucleotides are readily accessible for base pairing to complementary 3′ nucleotides of the target RNA (47,48).

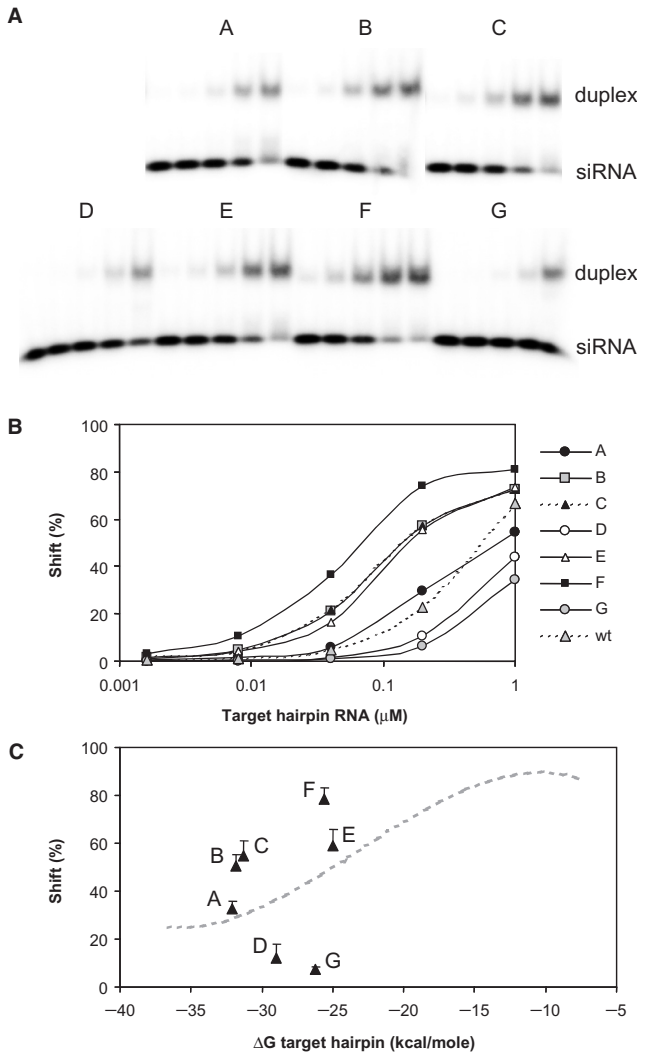

Figure 4. *In vitro* siRNA binding does not prefer an accessible 3′ end of the target. (**A**) Radioactively labeled oligonucleotide simulating the siRNA antisense strand (processed from shRNA-Pol) was incubated with increasing amounts of target variants A–G. SiRNA/target RNA duplex formation was analyzed by EMSA. (**B**) Free and bound siRNA oligonucleotide was quantified to calculate the level of duplex formation (bound siRNA/free + bound siRNA). (**C**) The thermodynamic stability of the target hairpins is plotted against the level of duplex formation with 0.2 μM target RNA. The gray dotted line represents the trendline observed in Figure 2C in the experiments with the initial set of mutants.

The importance of the target 3′ end was also revealed in experiments that selected for viruses that resist RNAi-mediated inhibition. We described a unique HIV-1 escape variant that acquired a mutation outside the 19-nt target, which forces the RNA into an alternative structure that occludes the 3′ end of the target (36).

Besides the *in vivo* RNAi measurements, we also tested the different RNA targets for their ability to interact with the siRNA *in vitro*. The overall ΔG effect of stable target hairpins is confirmed in this simplified *in vitro* setting, demonstrating that RNAi resistance is due to the inability of the siRNA to interact with the base-paired stem of the hairpin. We realize that the siRNA does not act by itself *in vivo* as it is part of RISC, of which the helicase activity may affect local structure in the target RNA (49). In fact, we observed an interesting discrepancy between the *in vivo* and *in vitro* results for the 5′/center/3′-destabilized hairpins. We observed that an accessible 3′ target is key for RNAi activity, but this effect was not seen *in vitro*. This result may indicate an important contribution of RISC in the siRNA-target RNA annealing step.

Thus, target RNA structure is an important factor when selecting a suitable target sequence, as it can have a negative effect on RNAi efficiency. For instance, it has been shown that the TAR hairpin of the HIV-1 genome is an unsuitable target because of its tight structure (31,40,50). On the other hand, it is obvious that an accessible sequence does not automatically make a good siRNA target (31), as the matching siRNA may not meet the criteria of an effective siRNA (51). It has been proposed to include a calculation of the amount of hydrogen bonds within the target sequence as a parameter for efficient target sequences (39). We provide a ΔG threshold at which an hairpin RNA structure becomes inaccessible, and we differentiate between different target positions. When designing antiviral siRNAs one may also consider ways to obstruct viral escape via folding of an alternative target RNA structure (36). The local RNA region should be screened for the absence of alternative foldings that occlude the 3′ end of the target and that can be selected by one or two mutations. If not available, the genetic threshold for structure-based escape might prove too high, even for a fast evolving virus like HIV-1.

RNA structure-mediated resistance against RNAi is in fact beneficial when expressing highly structured shRNAs or miRNAs in cells. For instance, the incorporation of shRNA cassettes in a lentiviral vector is potentially problematic, because the shRNA will target the viral RNA genome during vector production, thus reducing the titer. Such self-targeting has not been reported (52,53), we think because the target is not accessible as part of the perfectly base-paired shRNA hairpin. The apparent absence of such self-targeting is particularly important for the development of multi-shRNA lentiviral vectors without titer reduction. However, placing many tight RNA structures in the vector genome may negatively influence the titer by other means. For instance, reverse transcription is very sensitive to excessively stable RNA structure (54) and RNA polymerase II transcription may pause at sites where the RNA products folds stable hairpin structures (55). We did indeed observe that four shRNA cassettes reduce the lentiviral vector titer (ter Brake, unpublished data). Destabilizing the introduced shRNAs may avoid such vector problems, and provide additional benefits for cloning and sequencing of inverted repeat sequences (56). In our target model system, we mutated the antisense strand of the shRNA hairpin, leaving the sense target sequence intact. In the case of a true shRNA expression cassette, modifications will be made in the sense (target) strand to leave the guide/antisense siRNA strand unaltered. The obvious advantage will be reduced complementarity between the target and the siRNA inhibitor. The impact of such mutations on self-targeting is likely to depend on the position and type of mismatches

that are introduced (57,58). It is therefore impossible to make general rules for shRNA design and destabilization as each hairpin RNA structure will have its unique characteristics as target and effector in the RNAi mechanism. Here we demonstrate a ΔG window for shRNA-Pol destabilization without activating RNAi self-targeting, which may provide a guideline for other shRNAs. Positional effects should be considered, and hairpins may be destabilized to $\Delta G = -25$ kcal/mol as long as the target 3′ end remains base-paired. It is too early to define more general guidelines for structured RNA motifs other than the man-made, perfectly base-paired shRNA hairpins, as natural RNA structures differ significantly in their topology and architecture.

SUPPLEMENTARY DATA

Supplementary Data are available at NAR Online.

ACKNOWLEDGEMENTS

This research was sponsored by The Netherlands Organisation for Health Research and Development (ZonMw; VICI grant) and The Netherlands Organization for Scientific Research (NWO-CW; TOP grant). Funding to pay the Open Access publication charges for this article was provided by the VICI grant.

Conflict of Interest statement. None declared.

REFERENCES

1. Fire,A., Xu,S., Montgomery,M.K., Kostas,S.A., Driver,S.E. and Mello,C.C. (1998) Potent and specific genetic interference by double-stranded RNA in Caenorhabditis elegans. *Nature*, **391**, 806–811.
2. Vance,V. and Vaucheret,H. (2001) RNA silencing in plants-defense and counterdefense. *Science*, **292**, 2277–2280.
3. Waterhouse,P.M., Wang,M.B. and Lough,T. (2001) Gene silencing as an adaptive defence against viruses. *Nature*, **411**, 834–842.
4. Galiana-Arnoux,D., Dostert,C., Schneemann,A., Hoffmann,J.A. and Imler,J.L. (2006) Essential function in vivo for Dicer-2 in host defense against RNA viruses in drosophila. *Nat. Immunol.*, **7**, 590–597.
5. Kalmykova,A.I., Klenov,M.S. and Gvozdev,V.A. (2005) Argonaute protein PIWI controls mobilization of retrotransposons in the Drosophila male germline. *Nucleic Acids Res.*, **33**, 2052–2059.
6. Ketting,R.F., Haverkamp,T.H., van Luenen,H.G. and Plasterk,R.H. (1999) Mut-7 of C. elegans, required for transposon silencing and RNA interference, is a homolog of Werner syndrome helicase and RNaseD. *Cell*, **99**, 133–141.
7. Elbashir,S.M., Lendeckel,W. and Tuschl,T. (2001) RNA interference is mediated by 21- and 22-nucleotide RNAs. *Genes Dev.*, **15**, 188–200.
8. Hammond,S.M., Bernstein,E., Beach,D. and Hannon,G.J. (2000) An RNA-directed nuclease mediates post-transcriptional gene silencing in Drosophila cells. *Nature*, **404**, 293–296.
9. Zamore,P.D., Tuschl,T., Sharp,P.A. and Bartel,D.P. (2000) RNAi: double-stranded RNA directs the ATP-dependent cleavage of mRNA at 21 to 23 nucleotide intervals. *Cell*, **101**, 25–33.
10. Hammond,S.M., Caudy,A.A. and Hannon,G.J. (2001) Post-transcriptional gene silencing by double-stranded RNA. *Nat. Rev. Genet.*, **2**, 110–119.
11. Martinez,J., Patkaniowska,A., Urlaub,H., Luhrmann,R. and Tuschl,T. (2002) Single-stranded antisense siRNAs guide target RNA cleavage in RNAi. *Cell*, **110**, 563–574.
12. Filipowicz,W. (2005) RNAi: the nuts and bolts of the RISC machine. *Cell*, **122**, 17–20.
13. Brummelkamp,T.R., Bernards,R. and Agami,R. (2002) A system for stable expression of short interfering RNAs in mammalian cells. *Science*, **296**, 550–553.
14. Elbashir,S.M., Harborth,J., Lendeckel,W., Yalcin,A., Weber,K. and Tuschl,T. (2001) Duplexes of 21-nucleotide RNAs mediate RNA interference in cultured mammalian cells. *Nature*, **411**, 494–498.
15. Paul,C.P., Good,P.D., Winer,I. and Engelke,D.R. (2002) Effective expression of small interfering RNA in human cells. *Nat. Biotechnol.*, **20**, 505–508.
16. Holen,T., Amarzguioui,M., Wiiger,M.T., Babaie,E. and Prydz,H. (2002) Positional effects of short interfering RNAs targeting the human coagulation trigger Tissue Factor. *Nucleic Acids Res.*, **30**, 1757–1766.
17. Khvorova,A., Reynolds,A. and Jayasena,S.D. (2003) Functional siRNAs and miRNAs exhibit strand bias. *Cell*, **115**, 209–216.
18. Schwarz,D.S., Hutvagner,G., Du,T., Xu,Z., Aronin,N. and Zamore,P.D. (2003) Asymmetry in the assembly of the RNAi enzyme complex. *Cell*, **115**, 199–208.
19. Reynolds,A., Leake,D., Boese,Q., Scaringe,S., Marshall,W.S. and Khvorova,A. (2004) Rational siRNA design for RNA interference. *Nat. Biotechnol.*, **22**, 326–330.
20. Ui-Tei,K., Naito,Y., Takahashi,F., Haraguchi,T., Ohki-Hamazaki,H., Juni,A., Ueda,R. and Saigo,K. (2004) Guidelines for the selection of highly effective siRNA sequences for mammalian and chick RNA interference. *Nucleic Acids Res.*, **32**, 936–948.
21. Patzel,V., Rutz,S., Dietrich,I., Koberle,C., Scheffold,A. and Kaufmann,S.H. (2005) Design of siRNAs producing unstructured guide-RNAs results in improved RNA interference efficiency. *Nat. Biotechnol.*, **23**, 1440–1444.
22. Bohula,E.A., Salisbury,A.J., Sohail,M., Playford,M.P., Riedemann,J., Southern,E.M. and Macaulay,V.M. (2003) The efficacy of small interfering RNAs targeted to the type 1 insulin-like growth factor receptor (IGF1R) is influenced by secondary structure in the IGF1R transcript. *J. Biol. Chem.*, **278**, 15991–15997.
23. Kretschmer-Kazemi,F.R. and Sczakiel,G. (2003) The activity of siRNA in mammalian cells is related to structural target accessibility: a comparison with antisense oligonucleotides. *Nucleic Acids Res.*, **31**, 4417–4424.
24. Haasnoot,P.C.J. and Berkhout,B. (2006) RNA interference: its use as antiviral therapy. *Handbook of Experimental Pharmacology* Springer-Verlag Berlin Heidelberg, Heidelberg, Vol. 173, pp.117–150.
25. Coburn,G.A. and Cullen,B.R. (2002) Potent and specific inhibition of human immunodeficiency virus type 1 replication by RNA interference. *J. Virol.*, **76**, 9225–9231.
26. Jacque,J.M., Triques,K. and Stevenson,M. (2002) Modulation of HIV-1 replication by RNA interference. *Nature*, **418**, 435–438.
27. Lee,N.S., Dohjima,T., Bauer,G., Li,H., Li,M.J., Ehsani,A., Salvaterra,P. and Rossi,J. (2002) Expression of small interfering RNAs targeted against HIV-1 rev transcripts in human cells. *Nat. Biotechnol.*, **20**, 500–505.
28. Novina,C.D., Murray,M.F., Dykxhoorn,D.M., Beresford,P.J., Riess,J., Lee,S.K., Collman,R.G., Lieberman,J., Shankar,P. *et al.* (2002) siRNA-directed inhibition of HIV-1 infection. *Nat. Med.*, **8**, 681–686.
29. Banerjea,A., Li,M.J., Bauer,G., Remling,L., Lee,N.S., Rossi,J. and Akkina,R. (2003) Inhibition of HIV-1 by lentiviral vector-transduced siRNAs in T lymphocytes differentiated in SCID-hu mice and CD34+ progenitor cell-derived macrophages. *Mol. Ther.*, **8**, 62–71.
30. Boden,D., Pusch,O., Lee,F., Tucker,L. and Ramratnam,B. (2004) Efficient gene transfer of HIV-1-specific short hairpin RNA into human lymphocytic cells using recombinant adeno-associated virus vectors. *Mol. Ther.*, **9**, 396–402.
31. Das,A.T., Brummelkamp,T.R., Westerhout,E.M., Vink,M., Madiredjo,M., Bernards,R. and Berkhout,B. (2004) Human immunodeficiency virus type 1 escapes from RNA interference-mediated inhibition. *J. Virol.*, **78**, 2601–2605.
32. Lee,M.T., Coburn,G.A., McClure,M.O. and Cullen,B.R. (2003) Inhibition of human immunodeficiency virus type 1 replication in primary macrophages by using Tat- or CCR5-specific small interfering RNAs expressed from a lentivirus vector. *J. Virol.*, **77**, 11964–11972.

33. Lee,S.K., Dykxhoorn,D.M., Kumar,P., Ranjbar,S., Song,E., Maliszewski,L.E., Francois-Bongarcon,V., Goldfeld,A., Swamy,N.M. *et al.* (2005) Lentiviral delivery of short hairpin RNAs protects CD4 T cells from multiple clades and primary isolates of HIV. *Blood*, **106**, 818–826.
34. Ter Brake,O., Konstantinova,P., Ceylan,M. and Berkhout,B. (2006) Silencing of HIV-1 with RNA interference: a multiple shRNA approach. *Mol. Ther.*, **14**, 883–892.
35. Boden,D., Pusch,O., Lee,F., Tucker,L. and Ramratnam,B. (2003) Human immunodeficiency virus type 1 escape from RNA interference. *J. Virol.*, **77**, 11531–11535.
36. Westerhout,E.M., Ooms,M., Vink,M., Das,A.T. and Berkhout,B. (2005) HIV-1 can escape from RNA interference by evolving an alternative structure in its RNA genome. *Nucleic Acids Res.*, **33**, 796–804.
37. Berkhout,B. (2004) RNA interference as an antiviral approach: targeting HIV-1. *Curr. Opin. Mol. Ther.*, **6**, 141–145.
38. Westerhout,E.M., Ter Brake,O. and Berkhout,B. (2006) The virion-associated incoming HIV-1 RNA genome is not targeted by RNA interference. *Retrovirology*, **3**, 57–65.
39. Luo,K.Q. and Chang,D.C. (2004) The gene-silencing efficiency of siRNA is strongly dependent on the local structure of mRNA at the targeted region. *Biochem. Biophys. Res. Commun.*, **318**, 303–310.
40. Yoshinari,K., Miyagishi,M. and Taira,K. (2004) Effects on RNAi of the tight structure, sequence and position of the targeted region. *Nucleic Acids Res.*, **32**, 691–699.
41. Schubert,S., Grunweller,A., Erdmann,V.A. and Kurreck,J. (2005) Local RNA target structure influences siRNA efficacy: systematic analysis of intentionally designed binding regions. *J. Mol. Biol.*, **348**, 883–893.
42. Doench,J.G. and Sharp,P.A. (2004) Specificity of microRNA target selection in translational repression. *Genes Dev.*, **18**, 504–511.
43. Haley,B. and Zamore,P.D. (2004) Kinetic analysis of the RNAi enzyme complex. *Nat. Struct. Mol. Biol.*, **11**, 599–606.
44. Mathews,D.H., Sabina,J., Zuker,M. and Turner,D.H. (1999) Expanded sequence dependence of thermodynamic parameters improves prediction of RNA secondary structure. *J. Mol. Biol.*, **288**, 911–940.
45. Zuker,M. (2003) Mfold web server for nucleic acid folding and hybridization prediction. *Nucleic Acids Res.*, **31**, 3406–3415.
46. Lingel,A., Simon,B., Izaurralde,E. and Sattler,M. (2004) Nucleic acid 3′-end recognition by the Argonaute2 PAZ domain. *Nat. Struct. Mol. Biol.*, **11**, 576–577.
47. Ma,J.B., Yuan,Y.R., Meister,G., Pei,Y., Tuschl,T. and Patel,D.J. (2005) Structural basis for 5′-end-specific recognition of guide RNA by the A. fulgidus Piwi protein. *Nature*, **434**, 666–670.
48. Parker,J.S., Roe,S.M. and Barford,D. (2005) Structural insights into mRNA recognition from a PIWI domain-siRNA guide complex. *Nature*, **434**, 663–666.
49. Nykanen,A., Haley,B. and Zamore,P.D. (2001) ATP requirements and small interfering RNA structure in the RNA interference pathway. *Cell*, **107**, 309–321.
50. Brown,K.M., Chu,C.Y. and Rana,T.M. (2005) Target accessibility dictates the potency of human RISC. *Nat. Struct. Mol. Biol.*, **12**, 469–470.
51. Mittal,V. (2004) Improving the efficiency of RNA interference in mammals. *Nat. Rev. Genet.*, **5**, 355–365.
52. Nishitsuji,H., Ikeda,T., Miyoshi,H., Ohashi,T., Kannagi,M. and Masuda,T. (2004) Expression of small hairpin RNA by lentivirus-based vector confers efficient and stable gene-suppression of HIV-1 on human cells including primary non-dividing cells. *Microbes Infect.*, **6**, 76–85.
53. Van den Haute,C., Eggermont,K., Nuttin,B., Debyser,Z. and Baekelandt,V. (2003) Lentiviral vector-mediated delivery of short hairpin RNA results in persistent knockdown of gene expression in mouse brain. *Hum. Gene Ther.*, **14**, 1799–1807.
54. Beerens,N., Groot,F. and Berkhout,B. (2000) Stabilization of the U5-leader stem in the HIV-1 RNA genome affects initiation and elongation of reverse transcription. *Nucleic Acids Res.*, **28**, 4130–4137.
55. Hay,N. and Aloni,Y. (1984) Attenuation in SV40 as a mechanism of transcription-termination by RNA polymerase B. *Nucleic Acids Res.*, **12**, 1401–1414.
56. Miyagishi,M., Sumimoto,H., Miyoshi,H., Kawakami,Y. and Taira,K. (2004) Optimization of an siRNA-expression system with an improved hairpin and its significant suppressive effects in mammalian cells. *J. Gene Med.*, **6**, 715–723.
57. Du,Q., Thonberg,H., Wang,J., Wahlestedt,C. and Liang,Z. (2005) A systematic analysis of the silencing effects of an active siRNA at all single-nucleotide mismatched target sites. *Nucleic Acids Res.*, **33**, 1671–1677.
58. Holen,T., Moe,S.E., Sorbo,J.G., Meza,T.J., Ottersen,O.P. and Klungland,A. (2005) Tolerated wobble mutations in siRNAs decrease specificity, but can enhance activity in vivo. *Nucleic Acids Res.*, **33**, 4704–4710.
59. ter Brake, O., Berkhout B., Journal of Gene Medicine 2007 (in press). Lentiviral vectors that carry anti-HIV shRNAs: problems and solutions.